



Article

Recombinant Protein Production with *Escherichia coli* in Glucose and Glycerol Limited Chemostats

Anca Manuela Mitchell ^{1,†}, Valentina Gogulancea ^{2,†}, Wendy Smith ³, Anil Wipat ³ and Irina Dana Ofiteru ^{1,*}

¹ School of Engineering, Newcastle University, Newcastle upon Tyne NE1 7RU, UK; a.m.mitchell2@newcastle.ac.uk

² Centre for Sustainable Technologies, Ulster University, Newtownabbey BT37 0QB, UK; v.gogulancea@ulster.ac.uk

³ School of Computing, Newcastle University, Newcastle upon Tyne NE1 7RU, UK; wendy.smith@newcastle.ac.uk (W.S.); anil.wipat@newcastle.ac.uk (A.W.)

* Correspondence: dana.ofiteru@ncl.ac.uk; Tel.: +44-192-208-5618

† Equal contribution.

Abstract: Recently, there has been a resurgence of interest in continuous bioprocessing as a cost-optimised production strategy, driven by a rising global requirement for recombinant proteins used as biological drugs. This strategy could provide several benefits over traditional batch processing, including smaller bioreactors, smaller facilities, and overall reduced plant footprints and investment costs. Continuous processes may also offer improved product quality and minimise heterogeneity, both in the culture and in the product. In this paper, a model protein, green fluorescent protein (GFP) mut3*, was used to test the recombinant protein expression in an *Escherichia coli* strain with industrial relevance grown in chemostat. An important factor in enabling stable productivity in continuous cultures is the carbon source. We have studied the viability and heterogeneity of the chemostat cultures using a chemically defined medium based on glucose or glycerol as the single carbon source. As a by-product of biodiesel production, glycerol is expected to become a sustainable alternative substrate to glucose. We have found that although glycerol gives a higher cell density, it also generates higher heterogeneity in the culture and a less stable recombinant protein production. We suggest that manipulating the balance between different subpopulations to increase the proportion of productive cells may be a possible solution for making glycerol a successful alternative to glucose.

Keywords: *Escherichia coli*; recombinant protein production; chemostat; carbon source; flow cytometry



Citation: Mitchell, A.M.; Gogulancea, V.; Smith, W.; Wipat, A.; Ofiteru, I.D. Recombinant Protein Production with *Escherichia coli* in Glucose and Glycerol Limited Chemostats. *Appl. Microbiol.* **2021**, *1*, 239–254. <https://doi.org/10.3390/applmicrobiol1020018>

Academic Editor:
Ermenegilda Parrilli

Received: 31 May 2021
Accepted: 13 July 2021
Published: 16 July 2021

Publisher's Note: MDPI stays neutral with regard to jurisdictional claims in published maps and institutional affiliations.



Copyright: © 2021 by the authors. Licensee MDPI, Basel, Switzerland. This article is an open access article distributed under the terms and conditions of the Creative Commons Attribution (CC BY) license (<https://creativecommons.org/licenses/by/4.0/>).

1. Introduction

Recombinant protein production (RPP) has been steadily increasing since the 1980s, becoming a multi-billion dollar industry, with white and red biotechnology accounting for most of the market [1]. Bacterial expression systems are an attractive alternative to the more expensive or slow growing yeast or mammalian cell culture systems. *Escherichia coli* alone accounts for the production of 30–40% of proteins approved for therapeutic use [2]. Its well-characterised genome, the existence of many commercially available strains and their relatively low price, the high protein expression rates and the ease of performing genomic modifications to ensure high quality products explain the *E. coli* dominance amongst other microorganisms [1,3,4].

The switch from batch to continuous operation was also expected in, red biotechnology, to increase productivity, operational flexibility and the response to high market demands, following the trend demonstrated in the food, chemical and petrochemical industries. However, there was no such trend, and currently there are only a few continuous processes implemented using mammalian cells [3]. The use of microbial cells in continuous production modes at industrial scale remains uncommon, except for insulin production with *Saccharomyces cerevisiae* [5].

The most attractive characteristics of using continuous bioreactors (chemostats) are their high space–time yield, increased productivity, reduced protein production costs and lower space requirements. Moreover, in continuous bioreactors, the microorganisms' growth rate and the media composition (on which the protein production rate depends) are controlled to achieved “balanced growth” [6]. Thus, the optimisation of continuous cultures for RPP requires careful consideration of these two issues: the nutrient that limits growth and the microbial growth rate.

Continuous cultures should theoretically obtain products of more consistent quality than fed-batch processes [7]. Whereas in batch processing, product quality and productivity might be a trade-off, continuous biomanufacturing gives favourable recombinant protein characteristics [8]. In addition, chemostats allow for direct comparison between different experimental set-ups and eliminate some of the scale-up issues common for batch and fed-batch processes [9]. Nevertheless, most continuous culture studies have focused on the physiology of wild-type cells or low-stakes products such as ethanol. So far, no reports of industrial-scale continuous production of biopharmaceuticals using bacterial expression systems exist. The most-often-cited reasons for this are the genetic instabilities of the bacterial strains and recombinant plasmid leading to higher cell heterogeneity, the formation of inclusion bodies, and the increased acetate toxicity through overflow metabolism. Additionally, an increased metabolic burden which leads to lower growth rates and protein yield, and eventually increased cell death, as well as challenges of maintaining sterility, are also reported [10].

Previous studies have focused on quantifying the metabolic load associated with recombinant protein production [11,12] and determining the growth and protein production kinetics to optimise operating conditions and devise control strategies for the bioreactor [9]. High throughput techniques, including miniaturisation and parallelisation of bioreactors are used in both industry and research. Cascade operation and multistage culture that decouples the growth from the protein production stage have been investigated with promising results, combined with adequate induction strategies for protein expression [13,14].

The advances in continuous protein production using *E. coli* were recently summarised in [15], focusing on the knowledge transfer opportunities from fed-batch to continuous operation. One exciting development is using glycerol, a by-product of biodiesel production, as a substrate to make the RPP more sustainable [16–18]. Although there is an increased interest in the transition from fed-batch to continuous processing with *E. coli*, the heterogeneity of the culture and the lack of stable production are considered obstacles [15,19]. High-throughput single-cell expressions studies are required for understanding the dynamics and performance of heterogenous cell populations [20].

This work uses a model protein, green fluorescent protein (GFP) *mut3**, to test the recombinant protein expression in an *E. coli* strain with industrial relevance in glucose and glycerol-limited chemostats. A high throughput batch microbioreactor was used to select the best conditions for growth and protein production in the chemostat system. A chemically defined medium, with glucose or glycerol as the sole carbon source, was used as a feed solution and optimised for chemostat operation. We monitored the protein production and the heterogeneity of the cultures through flow-cytometry to compare the performance of the two carbon sources.

2. Materials and Methods

2.1. Strains

Two *E. coli* strains were used in this study: W3110 (*F*–*mcrA mcrB IN(rrnD- rrnE)1 λ*–), a wild-type strain with industrial applications; and CLD1301, which is derived from W3110 by transformation with the plasmid vector pD441-SR (containing the GFP-A gene). The vector has the following characteristics: a pUC ori allows autonomous replication in *E. coli* at a high copy number (500–700 plasmid copies per cell), which gives a high expression of the recombinant product; a kanamycin resistance cassette allows selection; and an

isopropyl β -D-1-thiogalactopyranoside (IPTG)-T5 inducible promoter allows modulating protein expression by varying the concentration of IPTG. We selected a wild strain and a recombinant one derived from it to have a baseline reference for the heterogeneity observed in chemostats. Easy quantification of the recombinant product was possible because of the high-level expression from the T5 promoter and reduced leakiness under the *lac* repressor. The strains were obtained from FUJIFILM Diosynth Biotechnologies (Billingham, UK) and are part of their culture collection used to explore basal expression and induction kinetics.

2.2. Growth Media and Culture Conditions

2.2.1. Growth Media

All cultures used the mineral medium reported in [21] supplemented with 20 $\mu\text{g L}^{-1}$ biotin and 50 $\mu\text{g/L}$ thiamine. In addition, 100 $\mu\text{L/L}$ Antifoam Y-30 (Sigma Life Sciences, St. Louis, MO), diluted 1/10 in deionised water, was added to prevent foaming. Kanamycin, in a final concentration of 50 $\mu\text{g/mL}$, was added for the growth of *E. coli* CLD1301 to select for plasmids.

The batch medium composition was well buffered with the phosphate salts, maintaining a pH of about 6.8 (starting value pH = 7) during fermentation. For the chemostat cultures the basal salts solution contained, per litre: 2.72 g KH_2PO_4 , 2.3 g NH_4Cl , 1.4 g $(\text{NH}_4)_2\text{SO}_4$, and 0.1 mL concentrated H_2SO_4 . The addition of concentrated H_2SO_4 lowered the pH to 3.5, allowing autoclaving at 121 °C for 30 min without forming derivatives from glucose or precipitations from phosphate salts. The vitamins and the antibiotic (for *E. coli* CLD1301) were added after autoclaving once the feed carboy cooled to room temperature.

In batch culture, different concentrations of glucose and glycerol were tested, while in continuous culture, the initial and the feed concentration of the carbon source were 4 g/L.

2.2.2. Culture Conditions

Batch cultures were performed in the BioLector[®] (m2p-labs, Baesweiler, Germany) microbioreactor, in 48-well FlowerPlates, operated as per the manufacturer's instructions. The experiments were run in triplicate and each run had one well with medium as internal plate standard negative control [14]. The FlowerPlate was covered with a gas-permeable sealing foil (F-GPR48-10, m2p-labs) to ensure aseptic conditions and reduced evaporation.

The following were maintained constant in all BioLector[®] fermentations: initial $\text{OD}_{600} \sim 0.05$, 800 μL filling volume, 1500 min^{-1} shaking frequency, 3 mm shaking diameter and 37 °C. The inoculation was made with cell stocks in the mid-exponential growth phase ($\text{OD}_{600} \sim 2$).

Biomass was measured as scattered light using an optical measuring unit (Fluostar, BMG Lab Technologies) with 620 nm excitation and no emission filter, located underneath the clear base of the FlowerPlate. Maximum growth rate μ_{max} was determined during the exponential phase, knowing its dependence on the natural logarithm of the biomass (A.U.). To investigate RPP in *E. coli* CLD1301, induction profiling was conducted with six different concentrations of IPTG (0, 0.05, 0.1, 0.25, 0.5 and 1 mM), added at the mid-exponential point of growth, at OD_{600} of 2. GFP concentration (A.U.) was measured online via fluorescence, with a 488 nm excitation and a 520 nm emission.

The average of 6–10 initial measurements for each biomass and fluorescence was subtracted from the totals to account for the signal originating from the medium background. Data were imported into Microsoft Excel for analysis. Gains were maintained constant across experiments, with a gain of 20 for biomass and a gain of 50 for GFP fluorescence. In the initial stages of fermentation at low biomass concentrations, few wells presented values smaller than the background; these were not removed from the data set.

Continuous cultures were performed in triplicate in 3 L computer-controlled jacketed bioreactors (eZ-Control, Applikon Biotechnology B.V.) with a 1.5 L working volume. The culture regime comprised of an initial batch phase, followed by a second chemostat phase. When $\text{OD}_{600} \sim 2$, at the mid-exponential point, the chemostat phase was initiated by activat-

ing the inlet and outlet peristaltic pumps. The inlet peristaltic pump, calibrated to operate at a set flow rate ($\frac{1}{2} \mu_{\max}$), controlled the specific growth rate in the chemostat.

The following parameters were maintained constant during bioreactor cultures: initial $OD_{600} \sim 0.05$, 1.5 L working volume, pH of 7, 37 °C temperature, 1 vvm air flow, 50 % dissolved oxygen saturation. A peristaltic pump dosing system with base mix (1M NaOH/1M KOH) and acid (1M HCl) maintained the pH at 7. The data were recorded with BioExpert software.

Chemostat conditions were reached after five volume changes and confirmed by constant biomass, a constant DO around set point and constant metabolic activity, evidenced by a constant alkali addition. The sampling times during the chemostat phase were every 2 h for the cultures on glucose and every 3 h for the cultures on glycerol. For inducing protein expression, IPTG was added in both the feed carboy and fermenter (concomitantly with switching from batch to continuous culture) to maintain a constant optimum inducer concentration during fermentation.

2.3. Sample Analysis

2.3.1. Biomass

Biomass was measured as OD_{600} (Jenway 6705 Spectrophotometer at 600 nm fixed wavelength) and total cell count (TCC) through flow cytometry (Attune Nxt Acoustic Focusing Cytometer, Life Technologies, Carlsbad, CA, USA). OD_{600} was calibrated against the cell dry weight (six calibration points between 0.25 and 2.5), but for this work we report the cell density as OD_{600} across all experiments [22].

2.3.2. Substrate Measurements

Glucose and glycerol concentrations in the filtered fermentation broth were determined using enzyme-based test kits (Megazyme International, Bray, Ireland) according to manufacturer's protocol. For the initial batch phase, the supernatant was diluted 1/10 in PBS before spectrophotometer measurements, while the steady-state supernatant obtained during the chemostat phase was not diluted.

2.3.3. Volatile Fatty Acids

Organic acids (formic, acetic and propionic) were quantified using an Dionex ICS-2100 ion chromatography system (Thermo Fisher Scientific, Sunnyvale, CA, USA) with a Dionex IonPac™ AG11-HC anion protection column. The reactor samples were filtered (Millex-GS syringe filter with 0.22 μm pore size) in the first two minutes after sampling to stop the bacterial activity and frozen immediately to -20 °C until further analysis.

2.3.4. Flow Cytometry

TCC, single-cell analysis of membrane integrity and RPP were assessed with Attune Nxt Acoustic Focusing Cytometer (Life Technologies, Carlsbad, CA, USA), equipped with a 488 nm laser. The SSC and FSC detectors were used to gate the population of interest. The green and red fluorescence were detected in the BL1 (BP 530/30) and BL2 channel (BP 574/26), respectively.

For membrane integrity the cells were stained with the cell-permeant thiazole orange (TO; fluorescence emission at 525 nm) and the cell-impermeant propidium iodide (PI; fluorescence emission at 623 nm) (final concentrations of 420 nmol/L and 43 $\mu\text{mol/L}$ for TO and PI, respectively) [23,24]. The percentage of cells that stain with either dye plotted as green over red fluorescence shows the number of viable (live) and dead cells.

In the presence of IPTG, the green fluorescence of the recombinant protein GFP mut3* replaces the TO staining. The strength of GFP mut3* lies in that the fluorophore forms from moieties from its polypeptide chain, requiring no co-factors for maturation other than oxygen and a 37 °C temperature. We confirmed through microscopy that the GFP-expressing cells displayed a single type of fluorescence and did not have the morphological aggregates encountered in inclusion bodies, showing that at 37 °C the protein was soluble in the cytoplasm (Supplementary Materials, Figure S1). Therefore, the emitted fluorescence

intensity was a direct readout of recombinant protein production. Dead cells and debris were eliminated from analysis using gating on FSC and SSC.

Single-cell analysis of changes in membrane potential indicative of bacterial stress was studied using a triple dye combination: bis-(1,3-dibarbituric acid)-trimethine oxonol (DIBAC₄₍₃₎; fluorescence emission at 525 nm), ethidium bromide (EB; fluorescence emission at 575 nm) and propidium iodide (PI; fluorescence emission above 630 nm), based on the method reported in [25]. The dyes were added to a final concentration of 10 µg/mL DIBAC₄₍₃₎, 10 µg/mL EB and 5 µg/mL PI. Stained cells were incubated for 30 min at 37 °C, in the dark, before flow cytometry analysis. Compensation was used to minimise fluorescence spill-over. The population was gated as active pumping cells that stained with neither of the dyes (DIBAC₄₍₃₎−, EtBr−, PI−), de-energised cells (DIBAC₄₍₃₎−, EtBr+, PI−), depolarised cells (DIBAC₄₍₃₎+, EtBr+, PI−) and dead cells (DIBAC₄₍₃₎+, EtBr−, PI+).

2.3.5. Data Acquisition and Analysis

All samples for flow cytometry analysis were diluted in PBS buffer to a final OD₆₀₀ ~ 0.25 before analysis. The sheath flow rate was 25 µL/min, 5 µL sample volume was selected as a stop for the assessment of viability (TO/PI) and protein production (GFP/PI) and 30 µL as a stop for membrane potential assessment (DIBAC₄₍₃₎/EB/PI). The flow cytometry data were recorded with Attune Cytometric Software v 3.1 and saved as Flow Cytometry Standard (.fcs) files, which were exported, gated and read at single-cell level with Matlab R2019b, using the fca-readfcs.m function, available on Matlab's File Exchange. Data were gated using an in-house written routine and exported to Excel, with flow cytometry readings expressed in arbitrary units (A.U.) and live/dead counts as percentages (%). The non-parametric Mann–Whitney *U* test was used for assessing the significance of the observed variation between the results obtained in different chemostat conditions (comparing OD₆₀₀, total cell count, and fractions of live, dead, depolarised and de-energised cells). Statistical analysis was performed with Minitab 18.

3. Results and Discussions

We first pre-screened the wild and recombinant strains in a high-throughput micro-bioreactor, testing various glucose/glycerol concentrations to determine the maximum concentration at which the carbon source limited bacterial growth. A single factor limitation in the medium allows for balanced growth (when cells attain the maximum growth rate possible for that particular medium) and is the only readily reproducible growth condition [26], which is a prerequisite for comparing the two substrates. The results, presented in Figure 1, indicated that for both glucose and glycerol, for this defined medium formulation, the limiting concentration for the carbon source was 4 g/L [21]. Exceeding this value, other components of the medium also became limiting.

To select the dilution rate for chemostat operation, we computed each bacterial strain's maximum growth rate for each substrate. The results and the ensuing sampling strategies are presented in Table 1. For *E. coli* CLD1301 grown on glucose as the sole carbon source, the batch fermentations in BioLector[®] showed a μ_{\max} of 0.37 h^{−1} but a growth rate recovery was observed in the continuous experiments, with a μ_{\max} of 0.67 h^{−1}. Dilution rates, corresponding to $\frac{1}{2} \mu_{\max}$ were 0.3 h^{−1} for glucose (residence time 3.33 h) and 0.25 h^{−1} for glycerol (residence time 3.96 h). Steady state was assumed after five residence times, when the culture optical density OD₆₀₀ was constant, which is more conservative than the usual three residence times reported in the literature [20]. Based on induction profiling in BioLector[®] with different IPTG concentration (see Section 2.2.2), we selected 1mM as the optimum inducer concentration in the chemostat (Supplementary Materials, Figure S2).

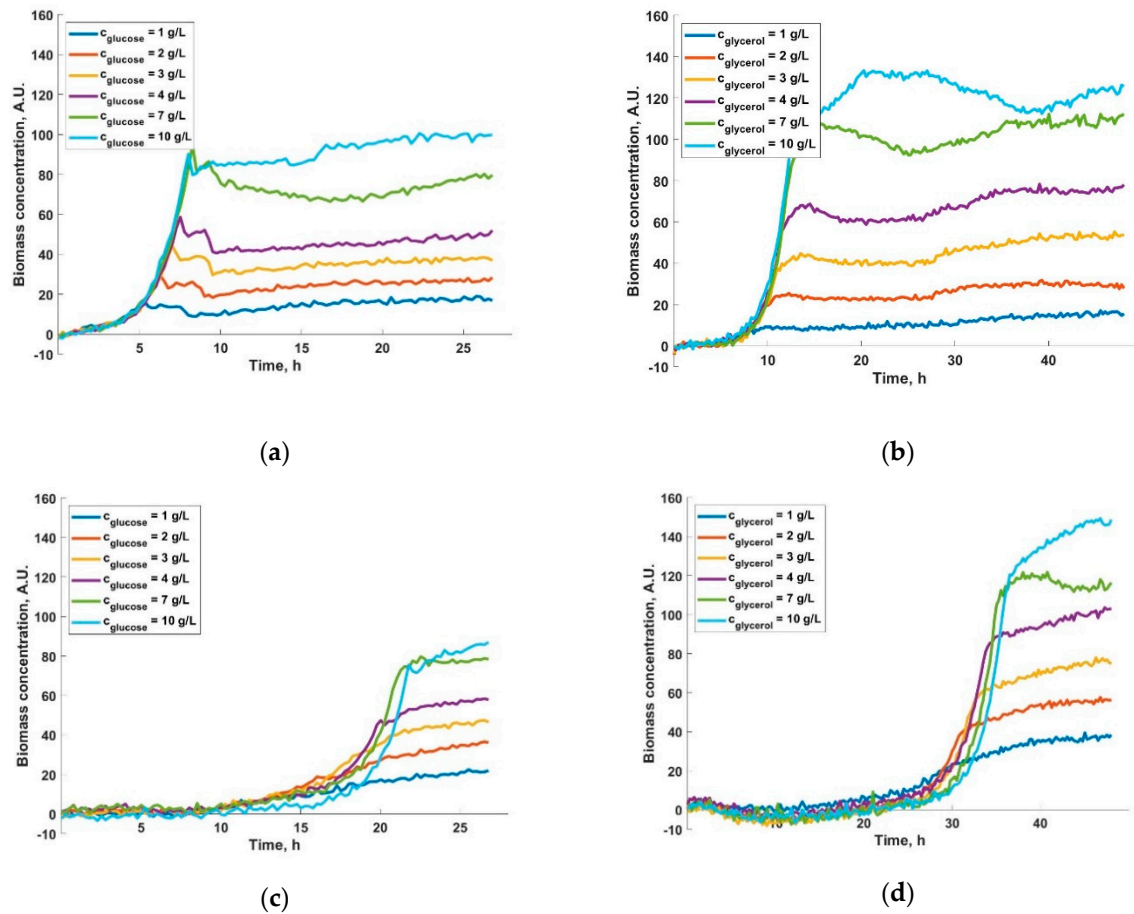


Figure 1. The influence of substrate concentration on *E. coli* W3110 grown on (a) glucose and (b) glycerol and on *E. coli* CLD1301 grown on (c) glucose and (d) glycerol. All cultures were run in triplicate in the batch microbioreactor BioLector[®]. Here we represent the mean of the three independent cultures. The standard deviation is not represented for these runs as, due to the multiple data points, the lines of different conditions would be undistinguishable.

Table 1. Maximum specific growth rates and sampling times for *E. coli* cultures on glucose and glycerol.

<i>E. coli</i> Strain	IPTG	Substrate	μ_{\max}	Sampling Times
W3110	0 mM	Glucose	0.6 h^{-1}	2 h
W3110	0 mM	Glycerol	0.5 h^{-1}	3 h
CLD1301	1 mM	Glucose	0.67 h^{-1}	2 h
CLD1301	1 mM	Glycerol	0.39 h^{-1}	3 h

To verify the suitability of glycerol compared to glucose for continuous RRP, we first analysed the performance of *E. coli* W3110 grown with and without IPTG addition. As expected from the BioLector[®] experiments, the optical density of the glycerol cultures was slightly higher compared with that for the glucose cultures (Figure 2a,b,e,f). However, this difference was not statistically significant for any of the two conditions studied (Mann–Whitney *U* test, $p > 0.05$). Previous reports indicated that glycerol has beneficial effects on the viability of cells compared to glucose [27]. Our results suggest that once steady state is reached glucose and glycerol are similar for biomass production, despite the longer culture time for the latter.

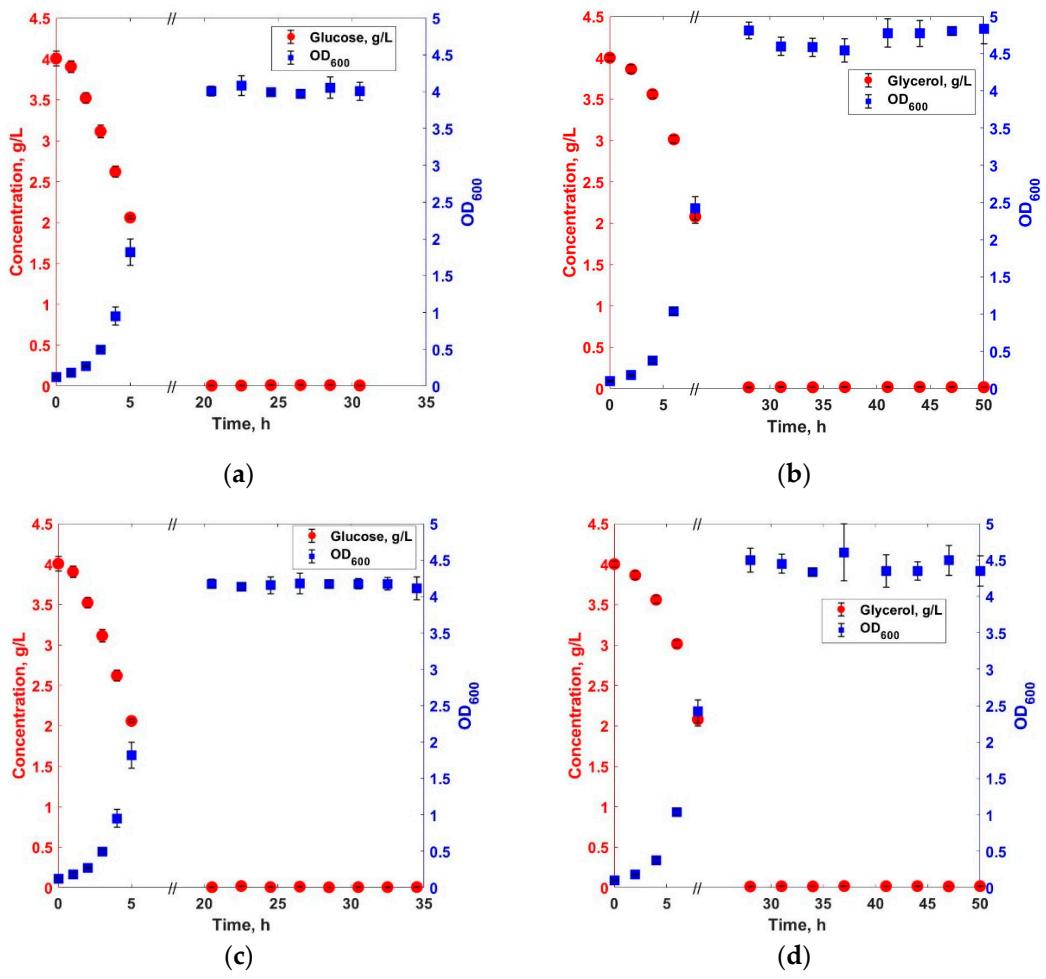


Figure 2. Cont.

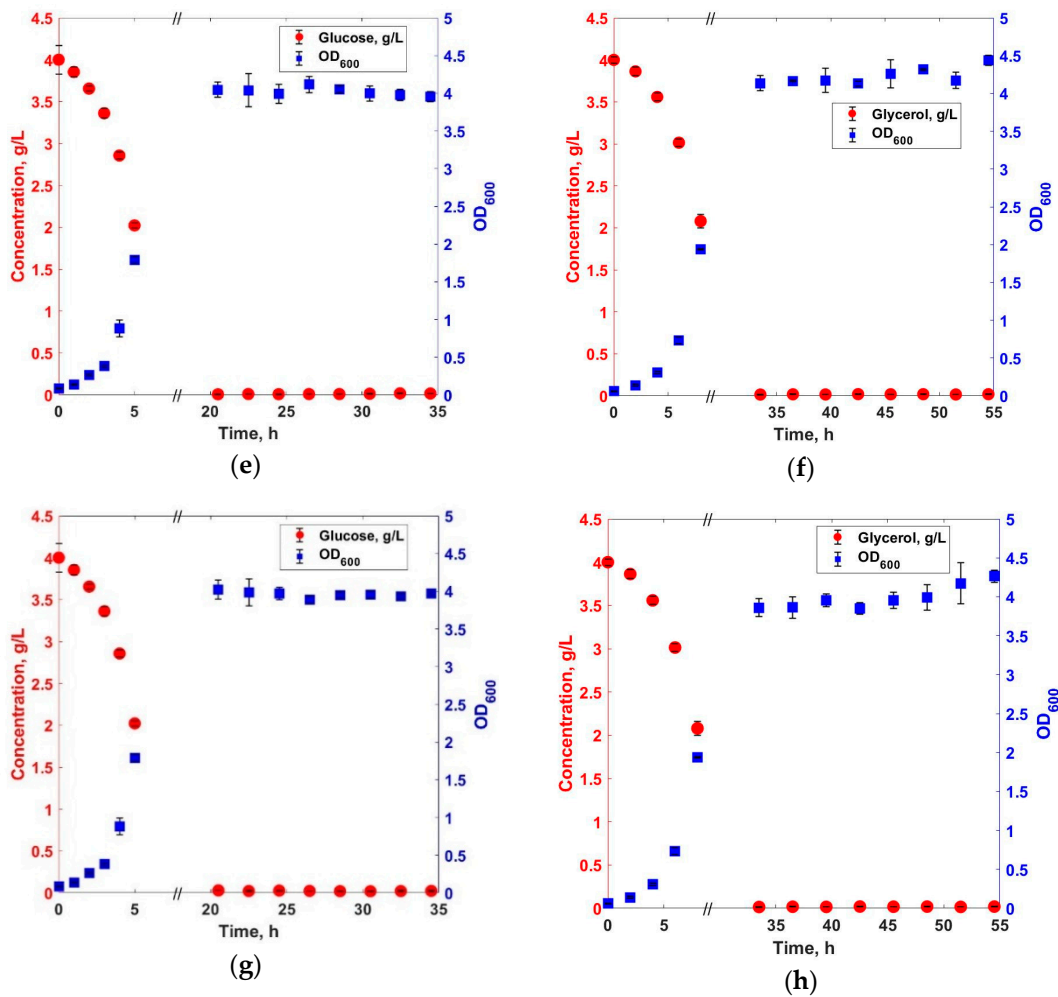


Figure 2. Substrate concentration and OD₆₀₀ measurements during chemostat culture of *E. coli* W3110 with no IPTG addition on (a) glucose and (b) glycerol, *E. coli* W3110 with 1mM IPTG grown on (c) glucose and (d) glycerol, *E. coli* CLD1301 with no IPTG addition grown on (e) glucose and (f) glycerol and *E. coli* CLD1301 with 1mM IPTG grown on (g) glucose and (h) glycerol. All cultures were run in triplicate.

Volatile fatty acids (formic, acetic and propionic), which are known to have negative effects on growth and to inhibit recombinant protein formation [28], had low concentrations in all cultures (Supplementary Materials, Figure S3). This confirms that the substrate concentrations and dilution rates were properly selected to prevent byproduct accumulation, which further shows the advantage of a chemostat system for recombinant protein production.

The addition of IPTG had no significant influence on the cell density (measured as OD₆₀₀) of *E. coli* CLD1301 grown on glucose or glycerol (Figure 2a,c,e,g for glucose; Figure 2b,d,f,h for glycerol). IPTG is known to be detrimental to cell growth and cellular viability of *E. coli* suspended cultures [29–32]. The chemostat runs results confirmed that the 1mM concentration selected for induction did not significantly influence cell growth (Mann–Whitney *U* test, $p > 0.05$).

More variation was observed in the cultures when measuring the cell density as TCC (Figure 3). TCC was slightly higher in the culture of *E. coli* W3110 on glycerol with and without IPTG, and the difference was statistically significant (Figure 3a,b,e,f; Mann–Whitney *U* test, $p < 0.05$). However, the percentage of live and dead cells between the two cultures was not statistically significant (Figure 3c,d,g,h; Mann–Whitney *U* test, $p > 0.05$) and for both substrates the percentage of live cells was maintained high.

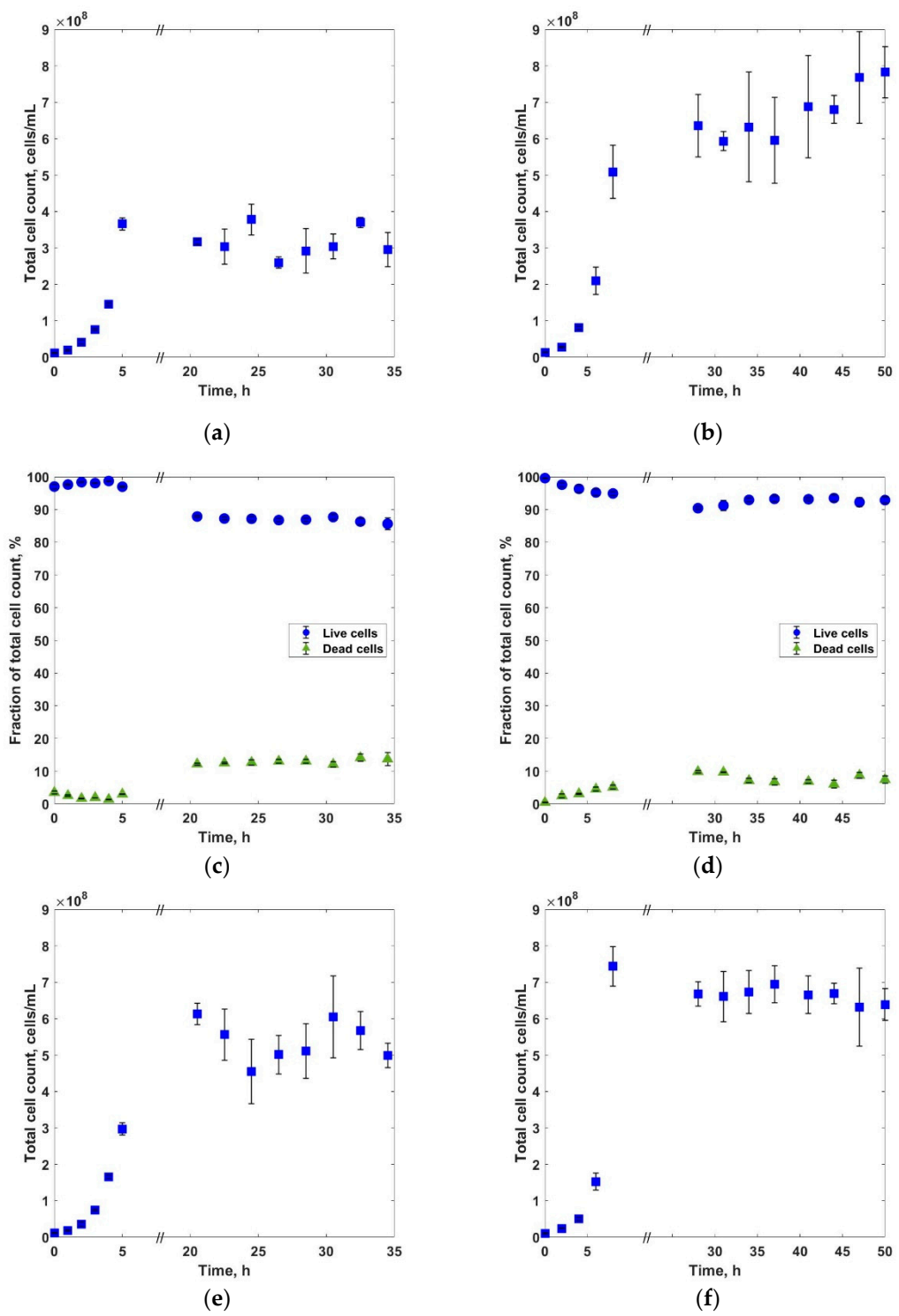


Figure 3. Cont.

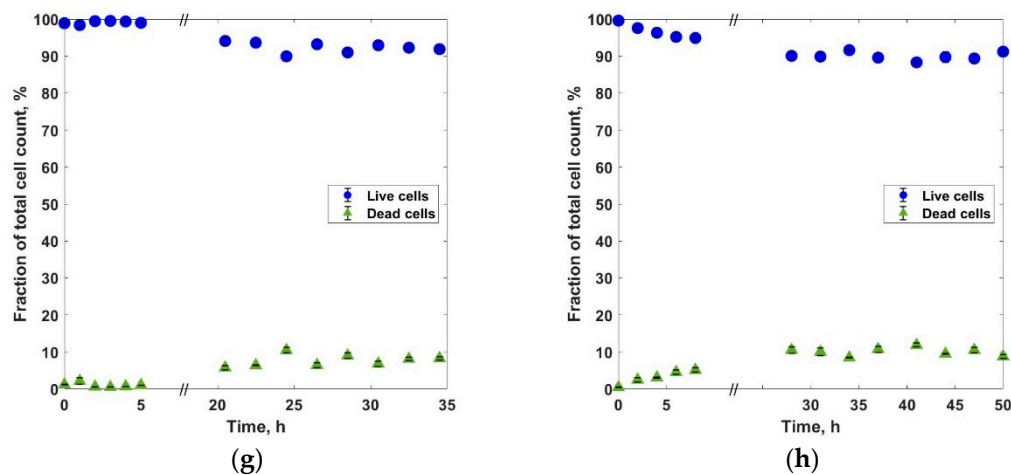


Figure 3. Total cell counts during culture of *E. coli* W3110 with no IPTG addition grown on (a) glucose and (b) glycerol, the fraction of live/dead cells during *E. coli* W3110 culture with no IPTG addition grown on (c) glucose and (d) glycerol, *E. coli* W3110 with 1mM IPTG grown on (e) glucose and (f) glycerol and the fraction of live/dead cells *E. coli* W3110 with 1mM IPTG grown on (g) glucose and (h) glycerol. All cultures were run in triplicate.

We further studied the stability of the cultures in the chemostat by measuring the changes in membrane potential, which is indicative of bacterial stress [33]. Samples collected after the bioreactor had reached steady state (and corresponding to the same sampling point as in Figure 2) were stained with a triple dye combination of DIBAC₄₍₃₎/ethidium bromide/PI. Primarily, all metabolically active cells with intact cytoplasmic membranes maintain membrane potential [34]. When membrane potential tends towards zero, the membrane is damaged, with ions travelling freely through it. This may not necessarily mean the cell is dead, but ‘compromised’ with decreased cellular functions, including biosynthesis of proteins and DNA, efflux pumping and respiration activity [35,36]. A membrane potential dye, DIBAC₄₍₃₎ is excluded from polarised cells that maintain membrane potential [37]. This means that well-energised (metabolically active) cells have low fluorescence DIBAC₄₍₃₎ staining. To further distinguish between the metabolically active populations, EB staining was applied. EB is used to assess the efflux pump activity, retained by cells with inactive efflux pump—‘de-energised’ population [38]; and pumped out of cells with functional efflux pumps—‘active’ population [39]. Cells that exhibit an increase in DIBAC₄₍₃₎ fluorescence intensity are considered to have undergone membrane depolarization, although the dye also stains ‘permeabilised’ cells with zero membrane potential. PI staining was applied to further distinguish between ‘depolarised’ and ‘permeabilised’ (dead) cells. The PI also displaces EB staining (which permeates all cell membranes and binds to RNA and DNA) in ‘permeabilised’ cells [35].

The heterogeneity in the cultures (measured as the variation in the percentage of active, depolarised, de-energised and dead cells) increased in the culture with glycerol as the carbon source (Figure 4). All but the percentages of depolarised and de-energised cells for *E. coli* W3110 (Figure 4a–d) differed significantly between the runs with glucose and with glycerol (Mann–Whitney *U* test, $p < 0.05$). Moreover, for *E. coli* CLD1301 grown on glycerol without the addition of IPTG (Figure 4d), the fraction of depolarised cells overpassed the one of active cells. This indicates that, despite the similar biomass production, the culture on glycerol generated higher heterogeneity in the *E. coli* population, which was likely to influence the recombinant protein production. A possible explanation for this behavior is the lower quality of glycerol as a carbon source (energetically), putting additional stress on the cells. It is possible that growing on glycerol, the *E. coli* culture is ‘hedging its bets’, developing several strategies to respond to the perceived starvation, which leads to greater heterogeneity [17]. Additional support for this assumption is the work of Liu et al. [40] who showed that as the quality of the substrate declines, cells express more genes in a ‘foraging effort’, looking for a better carbon source. Therefore, when using glycerol as

the carbon source, the trade-off between slightly higher biomass production and higher heterogeneity in the culture needs to be considered.

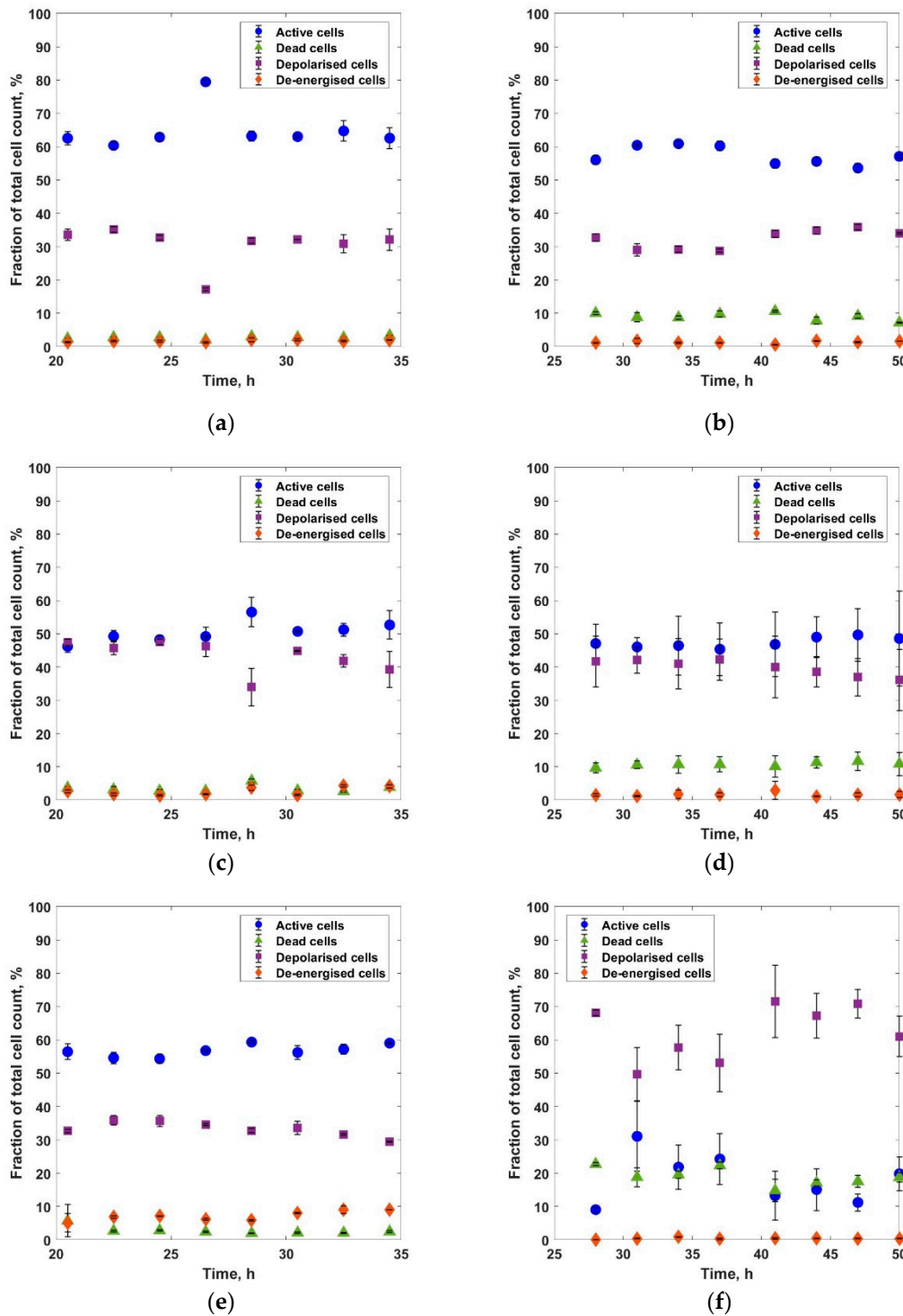


Figure 4. Dynamics of cell populations during steady state culture for (a) *E. coli* W3110 with no IPTG addition grown on (a) glucose and (b) glycerol, *E. coli* W3110 with 1mM IPTG grown on (c) glucose and (d) glycerol and *E. coli* CLD1301 with no IPTG addition grown on (e) glucose and (f) glycerol.

Due to the overlapping between the DIBAC₄₍₃₎ and GFP emission, this measurement could not be applied for the induced *E. coli* CLD1301.

Total cell count was slightly higher in the culture of *E. coli* CLD1301 on glycerol without IPTG, but the difference was not statistically significant (Figure 5a,b; Mann–Whitney *U* test, $p > 0.05$). However, we could see a significant increase in the percentage of dead cells compared with the culture on glucose (Figure 6c,d; Mann–Whitney *U* test, $p < 0.05$).

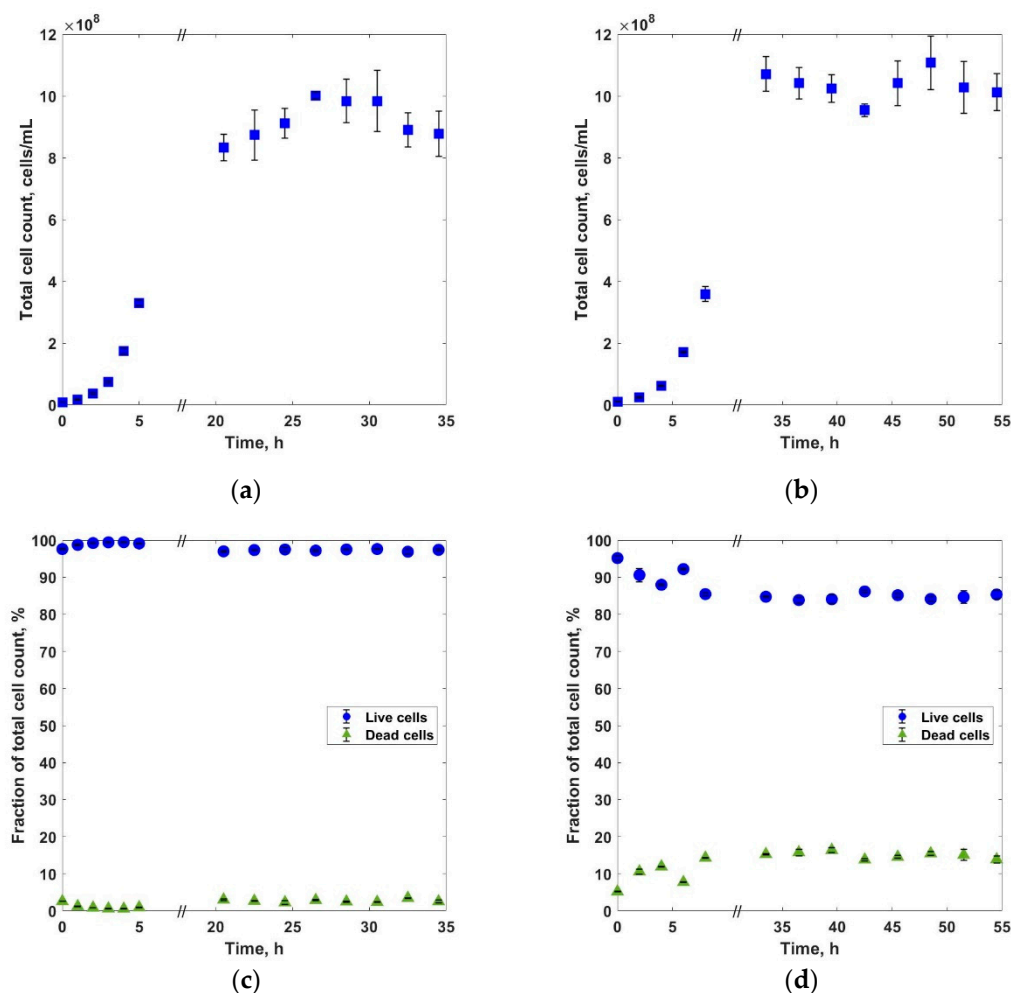


Figure 5. Total cell counts during culture of *E. coli* CLD1301 with no IPTG addition on (a) glucose and (b) glycerol and the fraction of viable/dead on (c) glucose and (d) glycerol. All cultures were run in triplicate.

For the induced *E. coli* CLD1301 culture, there was no significant difference for TCC and live/dead cells between the two substrates (Figure 6a–d; Mann–Whitney *U* test, $p > 0.05$) but the mean GFP fluorescence was lower for glycerol (Figure 6e,f; Mann–Whitney *U* test, $p < 0.05$). These results align with previous reports that mention glycerol carbon stress in the chemostat cultures of *E. coli* using glycerol as the carbon source [41].

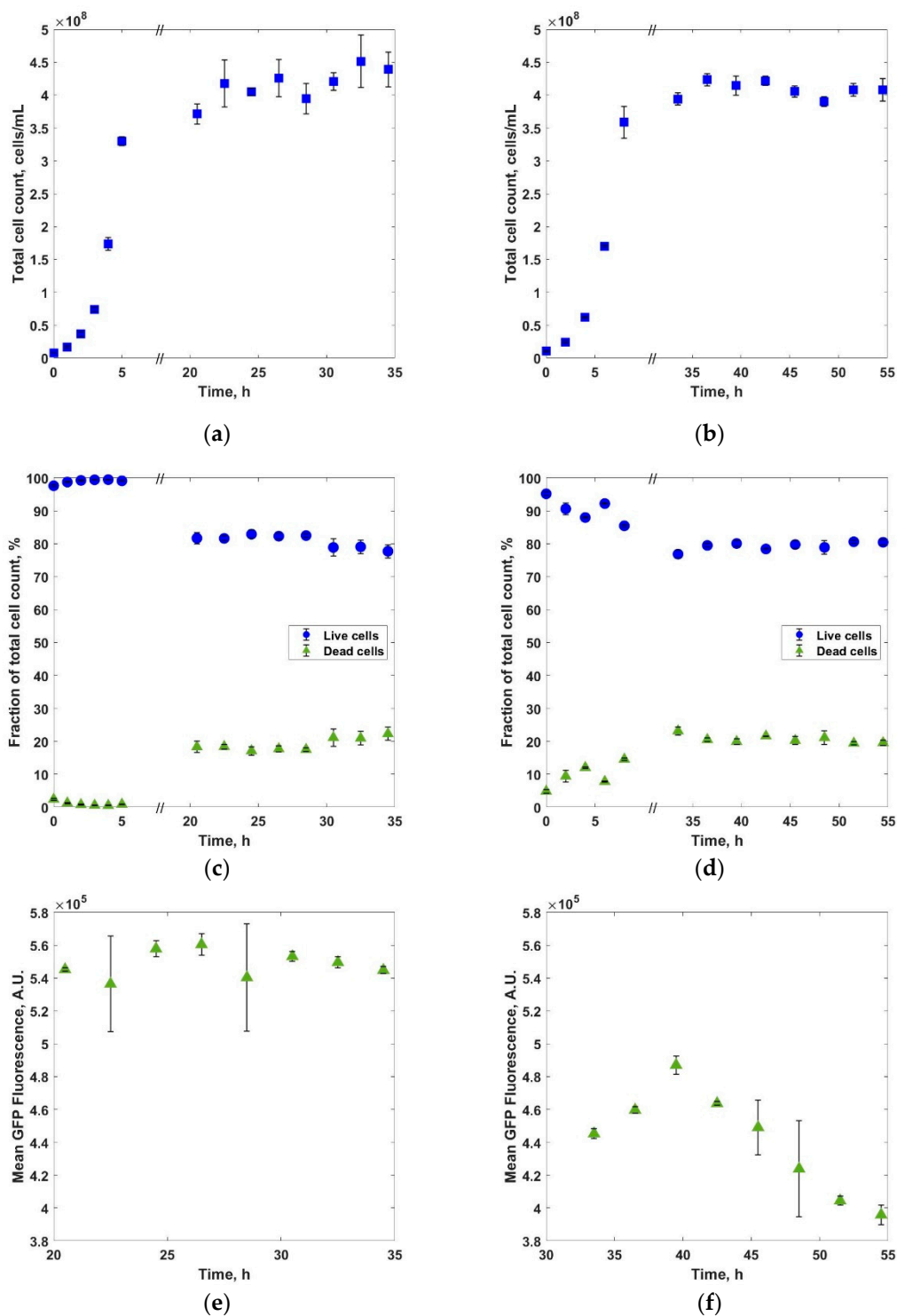


Figure 6. Total cell counts during culture of *E. coli* CLD1301 induced with IPTG grown on (a) glucose and (b) glycerol, fraction of live/dead cells during *E. coli* CLD1301 culture on (c) glucose and (d) glycerol and mean GFP fluorescence during *E. coli* CLD1301 culture on (e) glucose and (f) glycerol. All cultures were run in triplicate.

4. Conclusions

In this study, we compared continuous RPP in *E. coli* with glucose or glycerol as the sole carbon sources. Through single-cell analysis we could identify the different subpopulations in *E. coli* chemostat cultures, which revealed a higher heterogeneity than shown by TCC or OD₆₀₀. Our results indicate that the mean GFP fluorescence is lower, and

the protein production is less steady when the culture medium is based on glycerol. This partially confirms previous reports that heterogeneity in microbial production cell lines is detrimental for RPP [42]. We also note that glycerol gave a slightly higher overall biomass. Maintaining a higher biomass production and manipulating the balance between different subpopulations in order to increase the proportion of productive cells may be a possible solution for using glycerol as a successful alternative to glucose.

Reducing heterogeneity and promoting homogeneity is considered a good strategy for forcing cells into high productivity [43]. Nevertheless, heterogeneity is unavoidable and rather than looking to eliminate it, practitioners should consider managing it. We suggest that for a given substrate there is an optimal degree of heterogeneity in a bacterial population that corresponds to the best trade-off between the robustness of the fermentation process and productivity. In order to find this “sweet spot”, besides the high-throughput flow cytometry analysis [20], future work should include further analysis of the subpopulations monitored over a longer time period.

Supplementary Materials: The following are available online at <https://www.mdpi.com/article/10.3390/applmicrobiol1020018/s1>, Figure S1: Fluorescence microscope images of *E. coli* CLD1301 cells grown on glucose (a) and glycerol (b) induced with 1 mM IPTG and stained with propidium iodide (PI), Figure S2: The influence of IPTG concentration on biomass and GFP fluorescence for *E. coli* CLD1301 grown on (a) glucose and (b) glycerol. Figure S3: Volatile fatty acids concentrations.

Author Contributions: Conceptualization, I.D.O. and A.W.; methodology, I.D.O., A.M.M., W.S. and A.W.; data analysis, A.M.M. and V.G.; writing—original draft preparation, A.M.M. and V.G.; writing—review and editing, A.M.M., V.G., W.S., A.W. and I.D.O.; supervision, I.D.O. and A.W.; funding acquisition, I.D.O. All authors have read and agreed to the published version of the manuscript.

Funding: This research was funded by EPSRC through the DTA scholarship for A.M.M..

Data Availability Statement: All data generated and analysed during this study are included in this article. Raw datasets are available from the corresponding author on reasonable request.

Acknowledgments: The authors acknowledge the support of Andrew Fuller from the Newcastle University Flowcytometry Core Facility.

Conflicts of Interest: The authors declare no conflict of interest.

References

1. Tripathi, N.K.; Shrivastava, A. Recent developments in bioprocessing of recombinant proteins: Expression hosts and process development. *Front. Bioeng. Biotechnol.* **2019**, *7*, 420. [[CrossRef](#)]
2. Baeshen, M.N.; Al-Hejin, A.M.; Bora, R.S.; Ahmed, M.M.M.; Ramadan, H.A.I.; Saini, K.S.; Baeshen, N.A.; Redwan, E.M. Production of biopharmaceuticals in *E. coli*: Current scenario and future perspectives. *J. Microbiol. Biotechnol.* **2015**, *25*, 953–962. [[CrossRef](#)]
3. Steinebach, F.; Ulmer, N.; Wolf, M.; Decker, L.; Schneider, V.; Wälchli, R.; Karst, D.; Souquet, J.; Morbidelli, M. Design and operation of a continuous integrated monoclonal antibody production process. *Biotechnol. Prog.* **2017**, *33*, 1303–1313. [[CrossRef](#)]
4. Zhang, X.; Tervo, C.J.; Reed, J.L. Metabolic assessment of *E. coli* as a Biofactory for commercial products. *Metab. Eng.* **2016**, *35*, 64–74. [[CrossRef](#)]
5. Diers, I.V.; Rasmussen, E.; Larsen, P.H.; Kjaersig, I.L. Yeast fermentation processes for insulin production. *Bioprocess Technol.* **1991**, *13*, 166–176.
6. Egli, T. Microbial growth and physiology: A call for better craftsmanship. *Front. Microbiol.* **2015**, *6*, 287. [[CrossRef](#)]
7. Walther, J.; Lu, J.; Hollenbach, M.; Yu, M.; Hwang, C.; McLarty, J.; Brower, K. Perfusion cell culture decreases process and product heterogeneity in a head-to-head comparison with fed-batch. *Biotechnol. J.* **2019**, *14*, 1700733. [[CrossRef](#)]
8. Warikoo, V.; Godawat, R.; Brower, K.; Jain, S.; Cummings, D.; Simons, E.; Johnson, T.; Walther, J.; Yu, M.; Wright, B.; et al. Integrated continuous production of recombinant therapeutic proteins. *Biotechnol. Bioeng.* **2012**, *109*, 3018–3029. [[CrossRef](#)]
9. Peebo, K.; Neubauer, P. Application of Continuous Culture Methods to Recombinant Protein Production in Microorganisms. *Microorganisms* **2018**, *6*, 56. [[CrossRef](#)]
10. Croughan, M.S.; Konstantinov, K.B.; Cooney, C. The future of industrial bioprocessing: Batch or continuous? *Biotechnol. Bioeng.* **2015**, *112*, 648–651. [[CrossRef](#)]
11. Fragoso-Jiménez, J.C.; Baert, J.; Nguyen, T.M.; Liu, W.; Sassi, H.; Goormaghtigh, F.; Van Melderen, L.; Gaytán, P.; Hernández-Chávez, G.; Martínez, A.; et al. Growth-dependent recombinant product formation kinetics can be reproduced through engineering of glucose transport and is prone to phenotypic heterogeneity. *Microb. Cell Factories* **2019**, *18*, 1–16. [[CrossRef](#)]

12. Scott, M.; Gunderson, C.W.; Mateescu, E.M.; Zhang, Z.; Hwa, T. Interdependence of Cell Growth and Gene Expression: Origins and Consequences. *Science* **2010**, *330*, 1099–1102. [[CrossRef](#)]
13. Schmideder, A.; Weuster-Botz, D. High-performance recombinant protein production with *Escherichia coli* in continuously operated cascades of stirred-tank reactors. *J. Ind. Microbiol. Biotechnol.* **2017**, *44*, 1021–1029. [[CrossRef](#)]
14. Schmideder, A.; Cremer, J.H.; Weuster-Botz, D. Parallel steady state studies on a milliliter scale accelerate fed-batch bioprocess design for recombinant protein production with *Escherichia coli*. *Biotechnol. Prog.* **2016**, *32*, 1426–1435. [[CrossRef](#)]
15. Kopp, J.; Slouka, C.; Spadiut, O.; Herwig, C. The rocky road from fed-batch to continuous processing with *E. coli*. *Front. Bioeng. Biotechnol.* **2019**, *7*, 328. [[CrossRef](#)] [[PubMed](#)]
16. Slouka, C.; Kopp, J.; Strohmmer, D.; Kager, J.; Spadiut, O.; Herwig, C. Monitoring and control strategies for inclusion body production in *E. coli* based on glycerol consumption. *J. Biotechnol.* **2019**, *296*, 75–82. [[CrossRef](#)]
17. Martínez-Gómez, K.; Flores, N.; Castañeda, H.M.; Martínez-Batallar, G.; Hernández-Chávez, G.; Ramírez, O.T.; Gosset, G.; Encarnación, S.; Bolívar, F. New insights into *Escherichia coli* metabolism: Carbon scavenging, acetate metabolism and carbon recycling responses during growth on glycerol. *Microb. Cell Factories* **2012**, *11*, 46. [[CrossRef](#)]
18. Monteiro, M.R.; Kugelmeier, C.L.; Pinheiro, R.S.; Batalha, M.O.; César, A. Glycerol from biodiesel production: Technological paths for sustainability. *Renew. Sustain. Energy Rev.* **2018**, *88*, 109–122. [[CrossRef](#)]
19. Cabaleiro, R.G.; Mitchell, A.M.; Smith, W.; Wipat, A.; Ofițeru, I.D. Heterogeneity in Pure Microbial Systems: Experimental Measurements and Modeling. *Front. Microbiol.* **2017**, *8*, 1813. [[CrossRef](#)]
20. Heins, A.-L.; Johanson, T.; Han, S.; Lundin, L.; Carlquist, M.; Gernaey, K.V.; Sørensen, S.J.; Lantz, A.E. Quantitative Flow Cytometry to Understand Population Heterogeneity in Response to Changes in Substrate Availability in *Escherichia coli* and *Saccharomyces cerevisiae* Chemostats. *Front. Bioeng. Biotechnol.* **2019**, *7*, 187. [[CrossRef](#)]
21. Ihssen, J.; Egli, T. Specific growth rate and not cell density controls the general stress response in *Escherichia coli*. *Microbiology* **2004**, *150*, 1637–1648. [[CrossRef](#)]
22. Beal, J.; Farny, N.G.; Haddock-Angelli, T.; Selvarajah, V.; iGEM Interlab Study Contributors. Robust estimation of bacterial cell count from optical density. *Commun. Biol.* **2020**, *3*, 512. [[CrossRef](#)]
23. McHugh, I.O.L.; Tucker, A.L. Flow cytometry for the rapid detection of bacteria in cell culture production medium. *Cytom. Part A* **2007**, *71*, 1019–1026. [[CrossRef](#)]
24. Davey, H.M.; Kell, D.B. Flow cytometry and cell sorting of heterogeneous microbial populations: The importance of single-cell analyses. *Microbiol. Rev.* **1996**, *60*, 641–696. [[CrossRef](#)]
25. Caron, G.N.-V.; Stephens, A.W. Badley Assessment of bacterial viability status by flow cytometry and single cell sorting. *J. Appl. Microbiol.* **1998**, *84*, 988–998. [[CrossRef](#)]
26. Schaechter, M. A brief history of bacterial growth physiology. *Front. Microbiol.* **2015**, *6*, 289. [[CrossRef](#)]
27. Kopp, J.; Slouka, C.; Ulonska, S.; Kager, J.; Fricke, J.; Spadiut, O.; Herwig, C. Impact of Glycerol as Carbon Source onto Specific Sugar and Inducer Uptake Rates and Inclusion Body Productivity in *E. coli* BL21(DE3). *Bioengineering* **2017**, *5*, 1. [[CrossRef](#)]
28. Eiteman, M.; Altman, E. Overcoming acetate in *Escherichia coli* recombinant protein fermentations. *Trends Biotechnol.* **2006**, *24*, 530–536. [[CrossRef](#)]
29. Kosinski, M.J.; Rinas, U.; Bailey, J.E. Isopropyl- β -D-thiogalactopyranoside influences the metabolism of *Escherichia coli*. *Appl. Microbiol. Biotechnol.* **1992**, *36*, 782–784. [[CrossRef](#)]
30. Dvorak, P.; Chrast, L.; Nikel, P.I.; Fedr, R.; Soucek, K.; Sedlackova, M.; Chaloupkova, R.; De Lorenzo, V.; Prokop, Z.; Damborsky, J. Exacerbation of substrate toxicity by IPTG in *Escherichia coli* BL21(DE3) carrying a synthetic metabolic pathway. *Microb. Cell Factories* **2015**, *14*, 1–15. [[CrossRef](#)]
31. Malakar, P.; Venkatesh, K.V. Effect of substrate and IPTG concentrations on the burden to growth of *Escherichia coli* on glycerol due to the expression of Lac proteins. *Appl. Microbiol. Biotechnol.* **2012**, *93*, 2543–2549. [[CrossRef](#)]
32. Gomes, L.; Monteiro, G.; Mergulhão, F. The impact of IPTG induction on plasmid stability and heterologous protein expression by *Escherichia coli* biofilms. *Int. J. Mol. Sci.* **2020**, *21*, 576. [[CrossRef](#)]
33. Benarroch, J.; Asally, M. The Microbiologist’s Guide to Membrane Potential Dynamics. *Trends Microbiol.* **2020**, *28*, 304–314. [[CrossRef](#)]
34. Diaz, M.; Herrero, M.; Garcia, L.; Quirós, C. Application of flow cytometry to industrial microbial bioprocesses. *Biochem. Eng. J.* **2010**, *48*, 385–407. [[CrossRef](#)]
35. Nebe-Von-Caron, G.; Stephens, P.; Hewitt, C.; Powell, J.; Badley, R. Analysis of bacterial function by multi-colour fluorescence flow cytometry and single cell sorting. *J. Microbiol. Methods* **2000**, *42*, 97–114. [[CrossRef](#)]
36. Bridier, A.; Hammes, F.; Canette, A.; Bouchez, T.; Briandet, R. Fluorescence-based tools for single-cell approaches in food microbiology. *Int. J. Food Microbiol.* **2015**, *213*, 2–16. [[CrossRef](#)] [[PubMed](#)]
37. Davey, H.; Guyot, S. Estimation of Microbial Viability Using Flow Cytometry. *Curr. Protoc. Cytom.* **2020**, *93*, e72. [[CrossRef](#)]
38. Kim, H.T.; Choi, H.J.; Kim, K.H. Flow cytometric analysis of *Salmonella enterica* serotype Typhimurium inactivated with supercritical carbon dioxide. *J. Microbiol. Methods* **2009**, *78*, 155–160. [[CrossRef](#)] [[PubMed](#)]
39. Hewitt, C.J.; Nebe-Von-Caron, G. An industrial application of multiparameter flow cytometry: Assessment of cell physiological state and its application to the study of microbial fermentations. *Cytometry* **2001**, *44*, 179–187. [[CrossRef](#)]
40. Liu, M.; Durfee, T.; Cabrera, J.E.; Zhao, K.; Jin, D.J.; Blattner, F.R. Global Transcriptional Programs Reveal a Carbon Source Foraging Strategy by *Escherichia coli*. *J. Biol. Chem.* **2005**, *280*, 15921–15927. [[CrossRef](#)]

41. Kittler, S.; Kopp, J.; Veelenturf, P.G.; Spadiut, O.; Delvigne, F.; Herwig, C.; Slouka, C. The Lazarus *Escherichia coli* Effect: Recovery of Productivity on Glycerol/Lactose Mixed Feed in Continuous Biomanufacturing. *Front. Bioeng. Biotechnol.* **2020**, *8*, 993. [[CrossRef](#)] [[PubMed](#)]
42. Delvigne, F.; Goffin, P. Microbial heterogeneity affects bioprocess robustness: Dynamic single-cell analysis contributes to understanding of microbial populations. *Biotechnol. J.* **2013**, *9*, 61–72. [[CrossRef](#)] [[PubMed](#)]
43. Binder, D.; Drepper, T.; Jaeger, K.-E.; Delvigne, F.; Wiechert, W.; Kohlheyer, D.; Grünberger, A. Homogenizing bacterial cell factories: Analysis and engineering of phenotypic heterogeneity. *Metab. Eng.* **2017**, *42*, 145–156. [[CrossRef](#)] [[PubMed](#)]